

# The KMOS Redshift One Spectroscopic Survey (KROSS)

Richard Bower<sup>1</sup>  
Martin Bureau<sup>2</sup>

<sup>1</sup> Institute for Computational Cosmology,  
University of Durham, United Kingdom

<sup>2</sup> Sub-department of Astrophysics,  
University of Oxford, United Kingdom

on behalf of the KROSS consortium

A brief overview of the first results from KROSS, a VLT/KMOS guaranteed time programme is presented. KROSS will spatially resolve the dynamics, metallicity and star formation of 1000 mass- and colour-selected galaxies at  $z \sim 1$ . These data will chart the formation of disc galaxies at the epoch of peak star formation density in the Universe.

At redshift  $z \sim 1$ , the Universe is roughly half its present age and very different to the present day. In particular, the volume-averaged star formation density of the Universe is an order of magnitude larger than at  $z = 0$  (e.g., Lilly et al., 1996). Although recognisable, disc galaxies are just beginning to emerge from the chaos of the first few billion years of the Universe's history, their star formation rates, gas masses and (possibly) interaction rates are far higher than in today's quiescent galaxies.

The second-generation Very Large Telescope (VLT) instrument, the *K*-band Multi-Object Spectrograph (KMOS), is a near-infrared integral field spectrograph with a high multiplexing capability (Sharples et al., 2013). Its 24 integral field units (IFUs) allow maps of key astrophysical quantities to be created faster than ever before, and the near-infrared spectral coverage is particularly powerful to target the well-understood restframe optical wavelength range around  $z \sim 1$ . The KMOS Redshift One Spectroscopic Survey (KROSS) aims to understand the changes in galaxy properties through a ground-breaking, spatially resolved study of a large and representative sample of galaxies at this key epoch.

## Observational challenges of galaxy surveys

Within the past decade, there has been incredible progress in the study of galaxies in the redshift range  $1 < z < 2$ . A variety of techniques has been used to reliably disentangle distant galaxies from faint foreground objects, and the number of spectroscopically confirmed galaxies in this redshift range now numbers well into the tens of thousands. Restframe ultraviolet (UV) and optical colours, wide-area narrowband surveys and mid-infrared/submillimetre detections have all allowed observers to reliably determine galaxy stellar masses and quantify star formation rates. Although these data do not have the statistical power or quality of local surveys, such as the Sloan Digital Sky Survey (SDSS) or 2dF (Two-degree-Field Galaxy Redshift Survey; e.g., Abazajian et al., 2009; Colless et al., 2001), they do allow us to measure the evolution of stellar mass and to track black hole growth (e.g., Alexander & Hickox, 2012).

Recent studies have also made it possible to chart the dispersal of metals (e.g., Maiolino et al., 2008) and to begin to study the morphological and structural properties of galaxies as they settle onto a recognisable Hubble sequence (e.g., Swinbank et al., 2010). All these surveys have confirmed that the early Universe looks drastically different from its current state, and they have allowed us to begin to infer the formation histories of typical galaxies. At the highest redshifts however, massive galaxies are seen to be undergoing rapid star formation and the Hubble sequence is not yet in place.

Advances in observational surveys have been mirrored by progress in numerical simulations. In particular, models have highlighted the importance of high gas accretion at  $1 < z < 2$ . At these redshifts, even massive galaxies are continuously fed by narrow and cool “cold streams” of gas from the intergalactic medium (Dekel et al., 2009; van der Voort, 2011), promoting rapid but unstable star formation (e.g., Hopkins et al., 2012). As the Universe ages, these inflows become more tenuous and are eventually disrupted by outbursts from the black holes that grow at the centres of the emerging galaxies (e.g., Bower et al., 2006). By the

present day, these processes have led to the formation of a recognisable Hubble sequence. In the current generation of simulations, the emergence of the Hubble sequence arises because of the evolution of the fuelling rates of galaxies, and not because of a decline in the rate of galaxy merging (Behroozi et al., 2013).

Simulation results generally agree well with the global properties of the galaxy population, but they are intrinsically statistical in nature. With increasing survey speeds and growth in computational power, it is now possible to study the development of the internal properties of large samples of galaxies across these redshifts. Indeed, to enhance our empirical knowledge and refine theoretical models, the observational challenge must now be to quantitatively measure the internal structures of intermediate- and high-redshift galaxies across a range of masses and star formation rates (SFR). In this way, we will chart the growth of galaxy discs, comparing the growth of rotation speeds, disc stability and gas content against simulated galaxies.

With sufficient angular resolution, we can test whether secular processes in early systems play a significant role in building the majority of the  $z = 0$  stellar mass, and we can identify the key physical mechanisms producing the global trends observed at  $z = 0$  (e.g., Forster-Schreiber et al., 2009; Swinbank et al., 2012). Equally important, these constraints are vital to determine whether the numerical prescriptions developed to describe star formation in local galaxies can equally be applied to the dense and rapidly evolving interstellar medium of gas-rich, intermediate-redshift galaxies.

## KROSS

Some progress has been made in building samples of galaxies at  $z = 0.5$ – $1$  using the VLT Spectrograph for INTEGRAL Field Observations in the Near-Infrared (SINFONI) and the OH-Suppressing Infrared Integral Field Spectrograph (OSIRIS) on the Keck Telescope (e.g., Puech et al., 2008), but with its 24 simultaneous IFUs, KMOS is already revolutionising this field and allows us to rapidly build significantly larger and more representative galaxy

samples at these redshifts. Comparing the new data to those of local optical IFU surveys, such as the Sydney Australian Astronomical Observatory Multi-object Integral Field Spectrograph (SAMi) and the Mapping Nearby Galaxies instrument (MANGA), will reveal how the current Hubble sequence has emerged from the chaos of the early Universe. A key goal of our KMOS guaranteed time programme is to establish a large and well-defined statistical sample of galaxies at  $z \sim 1$ .

KROSS will create a database of 1000 spatially-resolved, mass-selected star-forming galaxies at the critical  $z \sim 1$  epoch. The sample size is large enough that the results can be divided into multiple bins of, e.g., stellar mass (ranging from  $10^{9.5}$  to  $10^{10.7} M_{\odot}$ ), SFR, rotation speed and environment. Within each bin it will be possible to quantify trends between residuals from galaxy scaling relations, and to correlate deviations in SFR with velocity asymmetry and disc warping, thus quantifying the response of the nascent discs to interactions, gas flows and internal instabilities. Hence we will determine the relative roles of nature and nurture (and their imprecise boundary) in driving the evolution of the cosmic SFR density.

The first pilot observations to test the feasibility of the survey were taken during KMOS Science Verification in July 2013, when we observed 39 galaxies at  $z = 0.84$  from the High Redshift (Z) Emission Line Survey (HiZELS) of the SSA22 field (Small Selected Area), for a total of 2 hours per configuration. All observations were taken in the YJ-band filter with a spectral resolution of  $R = 3500$ . We detected 30 of the targeted galaxies and measured their spatially resolved dynamics, metallicity and star formation rate (Sobral et al., 2013; Stott et al., 2014).

In Period 92, KROSS was allocated its first seven guaranteed nights to target the first 240 star-forming galaxies at  $z \sim 1$ . Target selection for the survey requires careful consideration. Selecting fainter galaxies makes it simple to fill all of the KMOS IFUs, but fainter (or more distant) galaxies are smaller and therefore less well-resolved spatially. While asymptotic rotation curves can be recovered by exposing for longer, this impacts on sur-

vey speed. For the target selection, we thus imposed an optimal K-band limit of  $K_{AB} = 22.5$  mag. Our aim is to obtain a mass-selected survey of the star-forming galaxy population, so we prioritised galaxies with blue colours ( $r-z < 1$ ). This is sufficient to include essentially all galaxies with significant star formation, but galaxies with redder colours are also included with a well-defined sampling rate.

### KROSS preliminary results

Each galaxy was observed for a total of 4.5 hours using ABA sequences (where A is on-source and B is sky, with one IFU from each spectrograph permanently dedicated to sky to improve the OH residual subtraction). Data reduction was carried out with SPARK (the Software Package for Astronomical Reductions with KMOS; Davies et al., 2013). As we are primarily interested in emission line properties, we find the instrument has excellent stability, and our observations are limited by sky noise rather than systematic sky residuals. In total, we detected 93% of the targets (with most non-detections corresponding to faint or passive galaxies), and derived spatially resolved velocity maps for 80% of the sample.

The main panel of Figure 1 shows a fraction of the data obtained in one observation. The right-hand panel shows the reduced two-dimensional spectra as they appear after correcting for instrumental effects and sky subtraction; the individual spatial slices are clearly visible. Strong emission lines are evident, including H $\alpha$ , [N II] and the [S II] doublet. Careful examination of the spectra immediately reveals spatial gradients in the line velocities (rotation) and ratios (abundance). Thumbnails on the left-hand side of Figure 1 show the corresponding velocity fields, colour-coded.

The power of KROSS lies in the speed with which it is possible to build up large samples of intermediate-redshift galaxies. In Figure 2, we show the dynamics of the  $\sim 200$  galaxies in our Period 92 sample with spatially resolved emission lines, the location of each postage stamp indicating the stellar mass and SFR of the target galaxy. The location of the “main sequence” of star-forming galaxies

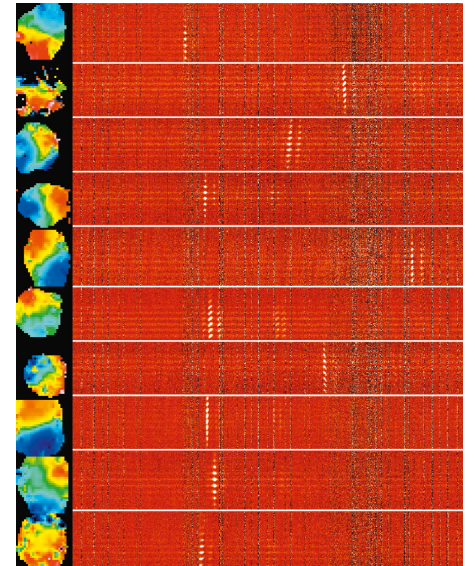


Figure 1. The main panel shows a fraction of the data obtained in a single KMOS observation of a field of  $z \sim 1$  galaxies. Strong emission lines are evident, as are the strong velocity and line ratio gradients across the galaxies. The left-hand side thumbnails are the corresponding velocity fields, colour-coded blue (negative velocity) and red (positive velocity) with respect to the galaxy systemic velocity.

at  $z \sim 1$  is illustrated by a dashed line (Karim et al., 2011).

Even a cursory examination of Figure 2 shows that the majority of the sample galaxies have disc-like kinematics, and that objects with strongly disturbed velocity fields are rare. However, the median ratio of the ionised gas rotation velocity to velocity dispersion  $v/\sigma$  (where  $\sigma$  is corrected for both instrumental broadening and beam smearing) is  $v/\sigma \sim 3$ , much lower than in local galaxies with a similar mass (where  $v/\sigma \sim 10$ ). Of course, local galaxies also have much lower specific SFRs, so these initial data already reinforce the idea that higher specific SFRs rates drive greater turbulence (or vice versa). Further analysis will allow us to determine if the change in gas mass agrees with the high fuelling rates of  $z \sim 1$  discs predicted in the simulations.

By combining the rotation and velocity dispersion maps, we can measure the fraction of rotationally supported systems in a mass-selected sample of  $z \sim 1$  galaxies, and use the Tully–Fisher relation to

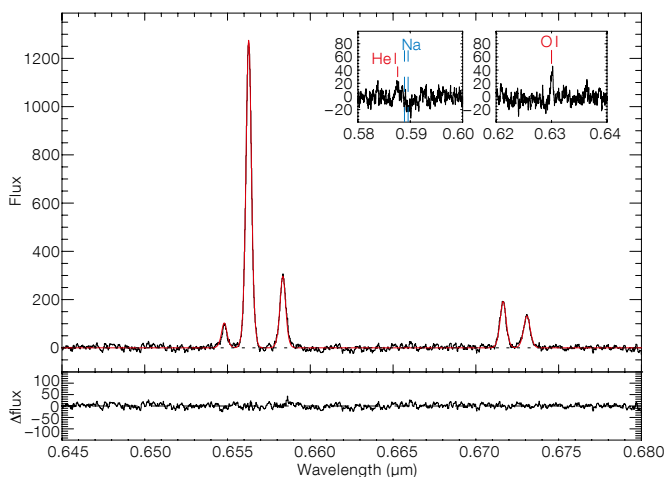
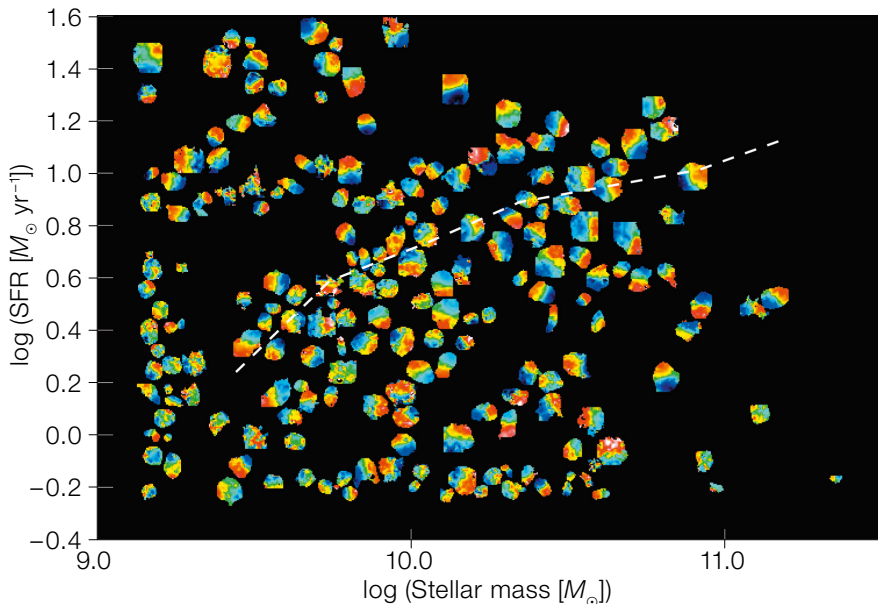


Figure 2. (Above) First results from KROSS, our KMOS guaranteed time survey of 1000 mass- and colour-selected galaxies at  $z \sim 1$ . The image shows the velocity fields of  $\sim 200$  galaxies with spatially resolved emission lines observed in Period 92, their position on the plot indicating their stellar mass and SFR, with the galaxy velocity fields colour-coded. The dashed line shows the location of the “main sequence” of star-forming galaxies at  $z \sim 1$  (Karim et al., 2011). Disc-like kinematics is seen in the majority of the sample.

Figure 3. Stacked spectrum of all KROSS galaxies from Science Verification and Period 92 observations that meet our selection criteria. The continuum was subtracted and the mean velocity of each galaxy spectrum was corrected before constructing the stack, and each spectrum was normalised

according to its reddening-corrected SFR before stacking. The insets show zooms around the [O I] 6300 Å emission line and the NaD 5995 Å absorption line. The lower panel shows the residuals from the best-fit model (red).

probe the evolution of the mass-to-light ratio of galaxies with redshift (e.g., Miller et al., 2013). We find that 80% of our targets rotate regularly, approximately twice the disc fraction at  $z \sim 2$  from the SINFONI Integral Field Spectroscopy (SINS) and the Assessing the Mass-Abundances Redshift (Z) Evolution (AMAZE) surveys (Shapiro et al., 2008; Contini et al., 2012). The ratio of stellar to dynamical mass suggests molecular

gas fractions of 30–60%, consistent with the evolution inferred from CO measurements between  $z = 0.4$  and 2 (e.g., Tacconi et al., 2013).

The good spectral resolution of KMOS also allows us to infer spatially resolved chemical abundance gradients (via the [N II] / H $\alpha$  ratio), that can be used to test “inside-out” vs. “outside-in” disc formation scenarios (Gilmore et al., 2002).

Finally, we can map the average properties of weaker spectral features by subtracting the local rotation velocities and then binning galaxies both spatially and as a function of stellar mass, SFR, etc. An example of such a stacked spectrum is shown in Figure 3, with the ambitious goal of searching for broad H $\alpha$  emission arising from outflowing gas (“super-winds”; e.g., Pettini et al., 2002). These features allow us to measure the mass and kinetic energy of the ejecta, presumably associated with star formation and/or active galactic nucleus driven feedback, one of the critical uncertainties in galaxy formation modelling.

KROSS data collection is progressing. By measuring the spatially resolved kinematics of  $\sim 1000$  galaxies at  $z \sim 1$ , this powerful database will provide deep insight into the different properties of galaxies when the Universe was half its current age, and those of similar mass galaxies today. We will move from asking whether the detailed properties of galaxies at these epochs differ, to understanding the internal mechanics of how and why.

#### Acknowledgements

The KROSS team would like to acknowledge STFC grants ST/I001573/1 and ST/H002456/1.

#### References

- Abazajian, K. et al. 2009, *ApJS*, 182, 543
- Alexander, D. M. & Hickox, R. C. 2012, *NewAR*, 56, 93
- Colless, M. et al. 2001, *MNRAS*, 328, 1039
- Dekel, A. et al. 2009, *Nature*, 457, 451
- Forster-Schreiber, N. et al. 2009, *ApJ*, 806, 1364
- Bower, R. et al. 2006, *MNRAS*, 370, 645
- Behroozi, P. et al. 2013, *ApJ*, 762, 31
- Contini, T. et al. 2012, *A&A*, 539, 91
- Davies, R. et al. 2013, *A&A*, 558, 56
- Gilmore, G. et al. 2002, *ApJ*, 574, 39
- Karim, A. et al. 2011, *ApJ*, 730, 61
- Lilly, S. et al. 1996, *ApJ*, 460, 1
- Maiolino, R. et al. 2008, *A&A*, 488, 463
- Miller, S. H. et al. 2013, *ApJ*, 762, 11
- Pettini, M. et al. 2002, *Ap&SS*, 281, 461
- Puech, M. et al. 2008, *A&A*, 484, 173
- Shapiro, K. L. et al. 2008, *ApJ*, 682, 231
- Sharples, R. et al. 2013, *The Messenger*, 151, 21
- Sobral, D. et al. 2013, *ApJ*, 779, 139
- Stott, J. et al. 2014, submitted, arXiv1407.1047
- Swinbank, M. et al. 2010, *MNRAS*, 405, 234
- Swinbank, M. et al. 2012, *MNRAS*, 436, 935
- Tacconi, L. et al. 2013, *ApJ*, 768, 74
- van de Voort, F. et al. 2011, *MNRAS*, 414, 2458